Program Digest, 2019 IEEE International Ultrasonics Symposium (IUS)
Glasgow, Scotland, October 6-9, 2019

Combining Quantitative 3D Subharmonic Imaging and Clinical Assessments for Accurate Characterization of Breast Masses

Flemming Forsberg,[1] Anush Sridharan,[1,2] Catherine W. Piccoli,[3] Alexander Sevrukov,[1] Annina Wilkes,[1] Haydee Ojeda-Fournier,[3] Robert F. Mattrey,[3] Priscilla Machado,[1] Maria Stanczak,[1] Daniel A. Merton,[1] Kirk Wallace,[5] and John R. Eisenbrey,[1]

[1]Department of Radiology, Thomas Jefferson University, Philadelphia, PA 19107, USA, [2]Department of Electrical and Computer Engineering, Drexel University, Philadelphia, PA 19104, USA, [3]South Jersey Radiology, Voorhees, NJ 08043, USA, [4]Department of Radiology, University of California San Diego, San Diego, CA 92103, USA and [5]GE Global Research, Niskayuna NY 12309, USA

Email: *flemming.forsberg@jefferson.edu*

***Abstract*—This multi-center study evaluated the ability of contrast-enhanced, nonlinear 3D ultrasound imaging to characterize indeterminate breast lesions using quantitative parametric maps and clinical assessments. In total 236 women with biopsy-proven breast lesions were enrolled in this study. Following B-mode and power Doppler imaging (PDI), an ultrasound contrast agent (Definity®, Lantheus Medical Imaging, N Billerica, MA, USA) was administrated. Contrast-enhanced 3D harmonic imaging (HI; transmitting/receiving at 5.0/10.0 MHz) as well as 3D subharmonic imaging (SHI; transmitting/receiving at 5.8/2.9 MHz) were performed using a modified Logiq 9 scanner (GE Healthcare, Waukesha, WI, USA) with a 4D10L probe. Five radiologists blinded to the reference independently scored the imaging modes using a 7-point BIRADS scale. Parametric volumes were constructed from time-intensity curves for vascular heterogeneity, perfusion (PER as the slope of the curve) and area under the curve (AUC) based on individual voxel values in the lesion. ROC analysis were applied to assess diagnostic accuracy with biopsy results as the reference. Out of the 236 cases, 219 were successfully scanned and biopsies resulted in 164 (75%) benign and 55 (25%) malignant lesions. 3D HI showed flow in 8 lesions (5 benign and 3 malignant), whereas 3D SHI visualized flow in 83 lesions (58 benign and 25 malignant). Hence, extracting quantitative parameters was restricted to the SHI volumes that demonstrated sufficient flow for processing. Diagnostic accuracy for the quantitative SHI parameters ranged from 0.52 to 0.75. Diagnostic accuracies from the clinical assessments ranged from 0.55-0.94 for baseline ultrasound, 0.52-0.93 for PDI, 0.59-0.85 for HI and 0.55-0.91 for SHI. The best logistical regression model achieved an accuracy of 0.91. In conclusion, combining quantitative SHI perfusion estimates and conventional B-mode imaging may increase the accuracy for characterizing indeterminate breast masses.**

Keywords—ultrasound; breast cancer; microbubbles; ultrasound contrast agents; subharmonic imaging

I. Introduction

Breast cancer is the second most common cancer in the world and the most frequent type of cancer among women (30% of all cancers). Experimental evidence suggests that breast cancer growth is dependent on angiogenesis [2]. Tumor angiogenesis is the development of a new, abnormal and leaky vascular network out of pre-existing vessels [3-5]. While mammography has high sensitivity in the detection of breast cancer, its low specificity results in a false-positive rate of roughly 80% [6], indicating the need for an adjunct imaging modality to improve characterization and reduce the number of unnecessary biopsies. Ultrasound imaging with microbubble based ultrasound contrast agents (UCAs) can provide both visualization and functional information related to the tumor microvasculature. Earlier studies by our group have validated the use of UCAs for imaging breast lesion vascularity [7, 8]. Contrast agent specific nonlinear imaging techniques provide the ability to delineate the vascularity from the surrounding tissue (since tissue primarily provides a linear response to the ultrasound signal).

This multi-center study evaluated the ability of contrast-enhanced, nonlinear 3D ultrasound imaging to characterize previously indeterminate breast lesions using quantitative parametric maps and clinical assessments.

II. Methods

A. Ultrasound imaging implementation

Imaging was performed on a modified Logiq 9 ultrasound scanner (GE Healthcare, Waukesha, WI, USA) with a 4D10L mechanically controlled linear array (bandwidth 3.5 – 11.0 MHz) capable of acquiring 3D volumes. The standard contrast harmonic imaging (HI) package was available on the scanner, and operated by transmitting 2 cycle pulses at 5 MHz (f_0) and receiving at 10 MHz ($2 \bullet f_0$). Subharmonic imaging (SHI) was implemented on the system by transmitting 4 cycle pulses at 5.8 MHz (f_0) and receiving at 2.9 MHz ($f_0/2$) [9]. Above a certain acoustic pressure threshold (typically > 200 kPa) and close to twice their resonance frequency the UCA microbubbles are able to generate a marked subharmonic frequency component (at half the transmit frequency). The subharmonic generation is specific to the UCA and does not occur in tissue. By selectively receiving at the subharmonic frequency it is possible to isolate vascular signals from tissue signals.

Supported by National Institutes of Health grant R01 CA140338, U.S. Army Medical Research Material Command grant W81XWH-11-1-0630 and Lantheus Medical Imaging (supplied Definity).

Pulse inversion was employed for both imaging modes to suppress any linear frequency components in the received signals. The mechanical index (MI) at maximum transmit settings was measured as 0.36 for 3D HI (peak negative pressure of 0.80 MPa) and 0.33 (peak negative pressure of 0.79 MPa) for 3D SHI [9].

B. Breast imaging procedures

The Institutional Review Boards of Thomas Jefferson University (TJU) and University of California, San Diego (UCSD) approved this study, which was conducted between January, 2011 and December, 2015. The study was compliant with the Health Insurance Portability and Accountability Act. Furthermore, this study was carried out under an FDA approved IND (no 112,241) and in accordance with ClinicalTrials.gov registration (NCT 01490892). Women (21 years or older) scheduled for a breast biopsy based on their clinical mammograms and/or B-mode ultrasound examinations were enrolled in the study after providing written informed consent. Baseline scans, consisting of 2D B-mode and power Doppler imaging (PDI) cine clips, were acquired first. These sweeps allowed for visualization of the tumor structure and vascularity along the tumor cross-section respectively.

Definity (Lantheus Medical Imaging, N Billerica, MA, USA) was the UCA used in this study. Definity was administered as a bolus injection via a 20-gauge catheter/needle placed in a peripheral vein on the forearm. For 3D HI, the UCA dosage was fixed at 0.25 mL, while 3D SHI used a weight-based dose of 20 μL/kg. Dosage for each of the imaging modes was selected based on previous imaging experience by our group [9]. The total dose (between HI and SHI) was limited to 1.5 mL (which is the total volume in a single vial of Definity). Each bolus injection was followed by a 10 mL flush of saline.

The 3D HI volume acquisition was started just before injection of Definity and continued until sufficient wash-out of the UCA (or 60 seconds). Imaging parameters were optimized on a case-by-case basis to minimize tissue signals, while simultaneously maintaining sufficient acoustic output to get a response from the bubbles. Next a 3D SHI volume acquisition was performed. A 10-15 minutes wait was observed between injections in order to allow for complete UCA wash out. Upon successful completion of the study, all files were transferred from the scanner to a desktop computer for offline analysis.

Following the ultrasound imaging study, all subjects underwent a breast biopsy (core or surgical). The pathology assessment of the biopsy specimens were used as the reference standard for this study.

C. Data analysis and image processing

Five experienced radiologists independently scored the four randomized, ultrasound imaging modes (B-mode, PDI, 3D HI and 3D SHI) using a 7-point BIRADS scale in which 1 indicated negative (i.e., no findings); 2, benign findings; 3, probably benign; 4, low suspicion of malignancy; 5, intermediate suspicion of malignancy; 6, moderate suspicion of malignancy and 7, highly suggestive of malignancy. The readers were blinded to the biopsy results and the cases were randomized as baseline (B-mode and PDI), baseline + HI, or baseline + SHI. There were 2 readers specific to each site (TJU & UCSD) and one overall reader (CWP) who assessed all the cases (a total of 3 readers/site).

Image processing and analysis was performed offline in MATLAB (2012a, The MathWorks Inc, Natick, MA, USA). Lesions that contained UCA flow were identified by a radiologist (10+ years of experience) in consensus with an ultrasound physicist 4DView (GE Medical Systems, Zipf, Austria). In cases with UCA flow, a region-of-interest (ROI) corresponding to the area of flow was created in 4DView. This ROI was projected through the entire 3D volume (i.e., across all the individual slices; Fig. 1). In order to generate a time-intensity curve (TIC) volume, the average image intensity within the ROI for each slice was calculated as a function of time. These intensity values were then used to generate a single TIC corresponding to that slice. This process was repeated for all 2D slices within the 3D volume. Finally, by merging the individual TICs for every 2D slice in the 3D volume, a single TIC volume was generated [10].

The TIC volumes were used to identify key time points corresponding to the UCA flow kinetics within the lesion [10]. These were, wash-in time (T_S: time point corresponding to start of UCA flow in the lesion), baseline (T_B: time point corresponding to 10% of peak UCA intensity along the TIC), peak (T_P: time point of peak UCA intensity), washout (T_W: time point of return to baseline UCA intensity), time-to-peak (TTP; time from T_B to T_P) and total transit time (TT; time from T_B to T_W). To analyze vascular heterogeneity throughout the lesion, the normalized change in UCA intensity from T_B to T_P for each TIC in the volume was measured as a distribution across the individual slices. Subsequently, the lesion volume was split into peripheral (defined as the outer third of the entire tumor area including 2 mm around the lesion boundary) and central sections to facilitate assessment of the variations in vascularity within the lesion in each area separately as well as for the ratio of the two areas.

To analyze the behavior of the vascularity with regard to kinetic parameters within the lesion, parametric volumes of the vascularity were developed. The parametric volumes were constructed based on two metrics; perfusion (PER; rate of change of UCA intensity from T_B to T_P) and area under the curve (AUC, sum of total UCA intensity from T_B to T_W). A single parametric value was generated for every voxel in the lesion volume from the volumes corresponding PER and AUC. These 3D parametric volumes were also broken down into the central, peripheral and the ratio of these two regions for diagnostic analysis.

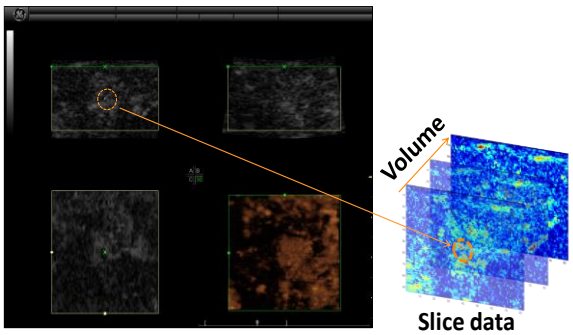

Fig. 1. An example of an ROI with contrast flow being mapped on to the raw 3D slice data as part of the volume processing.

D. Statistical analysis

Statistical analyses were performed using Stata 15.1 (StataCorp, College Station, TX, USA). Comparisons between malignant and benign lesions were performed using an unpaired *t*-test with a *p*-value of 0.05 or lower being considered statistically significant. ROC analysis and reverse, step-wise logistical regression were used to assess diagnostic accuracy (for individual parameters and in combination) with biopsy results as the reference standard, while the κ statistic was calculated for inter-reader agreement.

III. Results

A total of 236 patients were included in the study and image data were available for 219 cases. For the 17 cases that were not included in the final analysis, 8 cases were incomplete due to lack of access to a peripheral vein and 9 cases were incomplete due to technical malfunctions. Biopsies resulted in 164 (75%) benign and 55 (25%) malignant lesions. A significant difference was found between the mean age of patients with malignant (and benign lesions (56 vs. 49 years; p = 0.0027). Invasive ductal carcinomas (IDC) made up the majority of the malignant cases (42/55), while fibroadenomas (FA) were the most common type of benign lesion (51/164).

Vascularity was observed in 93 cases (69 benign and 24 malignant) with PDI, while UCA flow was observed in 8 lesions (5 benign and 3 malignant) for 3D HI and 83 lesions (58 benign and 25 malignant) with 3D SHI. Vascularity was better appreciated in 3D SHI than in 3D HI (qualitative assessment made by an ultrasound physicist and radiologist in consensus), due to the suppression of tissue signals. Given the poor performance of 3D HI in identifying vascularity, no additional image processing and analysis was performed on this group. There was no significant difference between 3D SHI and PDI in identifying lesions with vascularity (p = 0.52).

The overall assessment of the ability of contrast-enhanced, nonlinear 3D ultrasound imaging to characterize previously indeterminate breast lesions (i.e., for N = 219) resulted in accuracies from 0.81 to 0.84 (Fig. 2). When the ROC analysis was restricted to lesions with flow (i.e., for N = 83) there was no improvement in diagnostic accuracy (A_z from 0.82 – 0.83; Fig. 3). There were, however, marked differences between sites as shown in Tables 1 and 2. Inter-reader agreements were medium to low (κ<0.52).

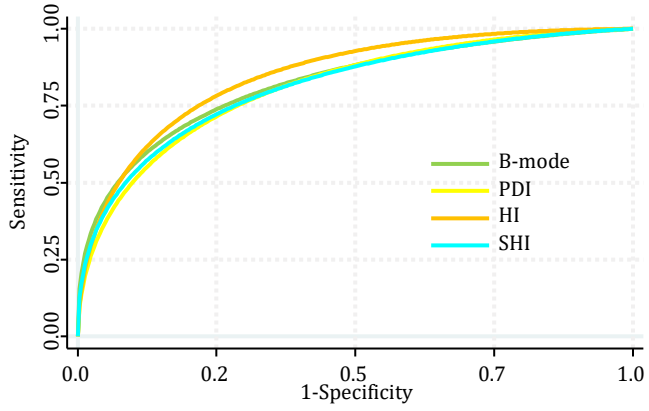

Fig. 2. ROC curves for characterizing all 219 breast lesions.

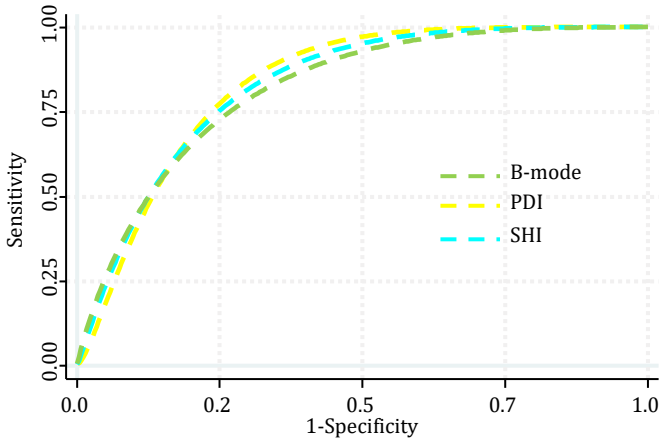

Fig. 3. ROC curves for characterizing the 83 breast lesions with flow.

TABLE 1. Diagnostic Accuracy (i.e., area under the ROC Curve – A_z) for UCSD (N = 56 for all; N = 18 for flow).

	B-mode		PDI		3D HI		3D SHI	
	all	flow	all	flow	all	flow	all	flow
R1	0.61	0.69	0.61	0.75	0.63		0.69	0.74
R2	0.55	0.61	0.57	0.52	0.63		0.61	0.55
R3	0.62	0.67	0.66	0.67	0.59		0.62	0.63

TABLE 2. Diagnostic Accuracy (i.e., area under the ROC Curve – A_z) for TJU (N = 156 for all; N = 65 for flow).

	B-mode		PDI		3D HI		3D SHI	
	all	flow	all	flow	all	flow	all	flow
R1	0.81	0.86	0.81	0.82	0.84		0.81	0.80
R2	0.88	0.94	0.88	0.93	0.85		0.85	0.91
R3	0.80	0.80	0.79	0.79	0.84		0.78	0.76

In order to determine the ability to characterize the breast lesions based on the quantitative 3D SHI parameters derived from the volume TICs, vascular heterogeneity, PER or AUC individual ROC curves were generated for the center, periphery and the ratio of the two. Diagnostic accuracies ranged from barely better than chance at 0.52 to a reasonable 0.75 (cf., Table 3). Finally, reverse, step-wise logistical regression models were constructed for the overall data as well as per site. Several combinations of parameters could completely resolve the breast masses from the smallest data-set (i.e., from UCSD). Overall and for 2 of the readers of the TJU data-set the optimal parameters in the logistical model were B-mode imaging and central PER. Hence, all the data were analyzed with a logistical regression model created from these two parameters (one clinical and one quantitative), which achieved very good A_z's ranging from 0.86 to 1.00. The ROC curves are shown in Fig. 4. The best overall logistical regression model achieved a 91% accuracy.

TABLE 3. DIAGNOSTIC ACCURACY (I.E., AREA UNDER THE ROC CURVE – A_z) FOR THE 3 QUANTITATIVE 3D SHI PARAMETERS.

	Vascular Heterogeneity	PER	AUC
Ratio	0.73	0.66	0.70
Central	0.70	0.69	0.75
Peripheral	0.52	0.73	0.65

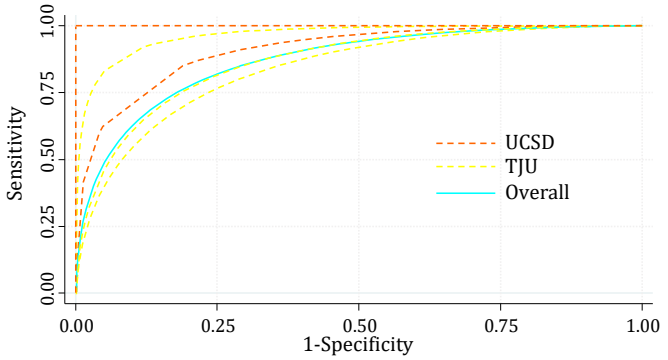

Fig. 4. ROC curves for the best logistical regression model overall as well as per site (A_z's ranged from 0.86 to 1.00).

IV. DISCUSSION

In this study, the ability to characterize indeterminate breast lesions using contrast-enhanced nonlinear ultrasound imaging was evaluated in 219 patients. 3D SHI proved to be better at visualizing flow in the lesions compared to 3D HI (in 83 vs. 8 cases, respectively). The numbers for 3D SHI were comparable to PDI (n = 93). Less than 5% of the 3D HI volumes showed any signs of UCA within the breast lesions, which was an extremely surprising finding. It is possible, that a combination of increased attenuation (at higher frequencies), weaker signal response and reduced sensitivity of transducer at this receive frequency contributed to the poor 3D HI performance in the breast. It is also important to note that there was a difference in the contrast dosages used for each of the modes (up to 5 times more for SHI). These dosages were selected based on previous *in vitro* and *in vivo* testing [9].

Clinical assessments of the 4 ultrasound imaging modes by 5 independent radiologists were performed and diagnostic accuracies were overall in the 81% to 84% range with markedly more variability at the sites (cf., Tables 1 and 2). Nine quantitative contrast enhanced vascularity measures (i.e., parameters associated with the angiogenic vessels 20 to 40 μm in diameter [7]) were investigated for breast lesion characterization. Individual accuracies ranged from 52% to 75%, which approaches a clinically useful measure. Encouragingly, the optimal logistical regression model (constructed from one clinical and one quantitative parameter) achieved an overall 91% diagnostic accuracy (i.e., an increase of over 16% from the quantitative parameters alone and approximately a 8% improvement over the radiologists' clinical readings).

V. CONCLUSION

In this study, the ability to use contrast-enhanced nonlinear ultrasound imaging, specifically SHI for visualizing and quantifying vascularity and subsequently characterizing previously indeterminate breast lesions was evaluated in a multi-center clinical trial. Results showed that 3D SHI is able to detect UCA flow in vascular lesions and performs better than 3D HI. Characterization of indeterminate breast lesions with quantitative 3D SHI parameters and clinical assessments improves diagnostic accuracy (with A_z reaching 0.86 to 1.00)

REFERENCES

[1] R. L. Siegel, K. D. Miller, A. Jemal, "Cancer Statistics, 2018", CA: a Cancer Journal for Clinicians, vol. 68 (1), 2018, pp. 7–30.

[2] J. Folkman, "What is the evidence that tumors are angiogenesis dependent?", Journal of the National Cancer Institute, vol 82 (1), 1990, pp. 4-7.

[3] D. M. McDonald and P. L. Choyke, "Imaging of angiogenesis: from microscope to clinic." Nature medicine, vol 9(6), 2003, pp. 713-725.

[4] W. W. Li, "Tumor angiogenesis: molecular pathology, therapeutic targeting, and imaging." Academic Radiology, vol 7(10), 2000, pp. 800-811.

[5] R. K. Jain, "Delivery of novel therapeutic agents in tumors: physiological barriers and strategies." Journal of the National Cancer Institute, vol 81(8), 1989, pp. 570-576.

[6] D. B. Kopans, Breast Imaging. Third edition. Philadelphia, PA, Lippincott Williams & Wilkins, 2007.

[7] F. Forsberg, et al., "Comparing contrast-enhanced color flow imaging and pathological measures of breast lesion vascularity." Ultasound in Medicine and Biology, vol 34(9), 2008, pp. 1365-1372.

[8] F. Forsberg, C. W. Piccoli, D. A. Merton, J. P. Palazzo, A. L. Hall, "Breast lesions: Imaging with contrast-enhanced subharmonic US—initial experience." Radiology, vol 244(3), 2007, pp. 718-726.

[9] J. R. Eisenbrey, et al., "Three-dimensional subharmonic ultrasound imaging in vitro and in vivo." Academic Radiology, vol 19(6), 2012, pp. 732-739.

[10] A. Sridharan, et al., "Quantitative analysis of vascular heterogeneity in breast lesions using contrast-enhanced three-dimensional harmonic and subharmonic ultrasound imaging." IEEE Transactions on Ultrasonics Ferroelectrics and Frequency Control, vol. 62(3), 2015, pp. 502–510.